

## Monte Carlo Code for the Study of Electron-Solid Interactions

Károly TÖKÉSI\* and Takeshi MUKOYAMA\*\*

*Received July 19, 1994*

A Monte Carlo code for calculating the electron-solid interaction processes has been developed. The individual scattering processes are taken into account in the calculation. We demonstrated that the backscattered electron spectrum for Al near the elastic peak calculated with the present code is in good agreement with the experimental result.

KEY WORDS: Electron transport/ Monte Carlo method/ Solid target

### 1. INTRODUCTION

In the last several years the study of the inelastic collision processes in the frame of the electron-solid interactions is in the center of the interest. A quantitative description of the spectra of electrons in keV region after scattering processes from solid is interesting in different fields of electron spectroscopy. Because of a large number of scattering events in solids and variety of scattering processes, analytical treatments are in general difficult and the Monte Carlo (MC) method, which simulates the electron scattering process with random numbers, is often used.

A variety of MC simulation methods for electron scattering have been developed and described in different papers.<sup>1-8)</sup> The computer codes based on these models have been successfully used for electron transmission and backscattering in solids. The conventional method to estimate electron energy-loss spectra is based on the continuous-slowing-down approximation,<sup>9)</sup> where the average rate of energy loss is estimated by the Bethe stopping power theory. However this approximation is inadequate to reproduce the fine structure in the energy spectrum of backscattered electrons near the elastic peak, because electrons occasionally lose a large fraction of their energy in a single collision and are deflected with a large scattering angle. In such a case, the most realistic model is the direct simulation method to trace the individual scattering event.

In the present work, an MC code has been developed and tested to study electron-solid interaction processes. The program is based on the algorithm similar to that of Shimizu *et al.*<sup>1)</sup> The trajectories of the primary electron and of the created secondary electrons are traced in the solid. Our main aim is to define the complete inelastic processes which can yield the magnitudes

\* Institute of Nuclear Research of the Hungarian Academy of Sciences (ATOMKI), H-4001 Debrecen, Hungary.

\*\* 向山 毅: Division of States and Structures, Institute for Chemical Research, Kyoto University, Uji, Kyoto, 611 Japan.

and the shapes of the energy-loss peaks close to the elastic peak in the backscattered electron spectrum. Our special interest lies in the energy region below 100 eV from the elastic peak. In this region the calculation is very sensitive to the computational model used and therefore it is a good test for a new computer code. The test calculation has been made for the energy spectrum of electrons backscattered from Al metal at 5-keV incident energy and compared with the experimental spectrum.

## 2. MONTE CARLO METHOD

The present Monte Carlo calculation is based on the screened Rutherford formula for elastic scattering, the excitation by Gryzinski for core electrons,<sup>10)</sup> the Streitwolf excitation function for conduction electrons,<sup>11)</sup> and the mean free path formula of Quinn for the bulk and surface plasmon excitation.<sup>12)</sup> Figure 1 shows schematically the present model for MC simulation of electron penetration in solids.

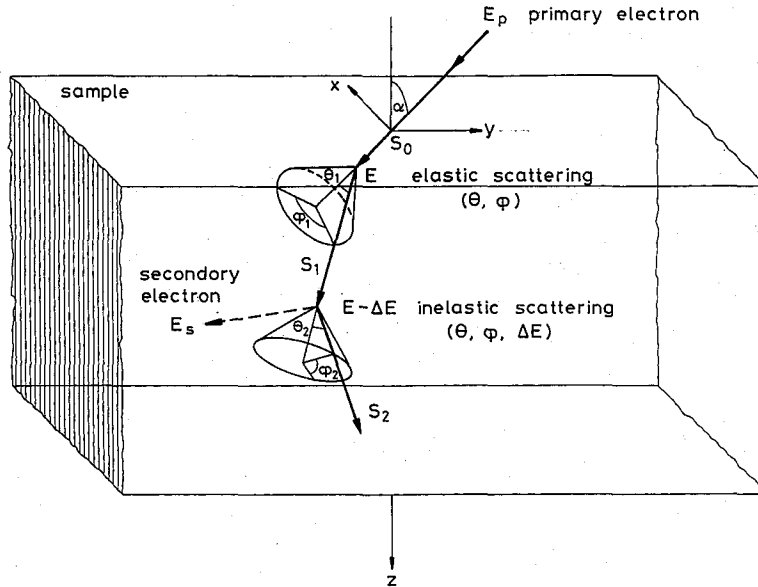


Fig. 1. Schematic drawing to illustrate the present model for Monte Carlo simulation of electron penetration in solids.

### 2.1 Elastic Scattering

The screened Rutherford scattering formula is written by<sup>13)</sup>

$$\frac{d\sigma}{d\Omega} = \frac{Z^2 e^4}{4E^2 (1 - \cos \Theta + 2\beta_N)^2}, \quad (1)$$

where  $Z$ ,  $\Theta$ ,  $e$  and  $E$  are the atomic number, the scattering angle, the charge of the electron, and the kinetic energy of the electron, respectively. The atomic screening parameter derived by Wenzel,<sup>13)</sup>  $\beta_N$ , is defined as

$$\beta_N = \frac{3.4Z^{2/3}}{E}. \quad (2)$$

The total elastic cross section as a function of electron energy,  $\sigma_e$ , is obtained by integrating Eq. (1) over all possible scattering angles and can be written as

$$\sigma_e = \frac{\pi Z^2 e^4}{4E^2 \beta(\beta+1)}. \quad (3)$$

The scattering angle  $\Theta$  of an individual elastic collision is determined by the use of a uniform random number  $R_1 \in (0, 1)$ :

$$R_1 = 2\pi \int_0^\Theta \frac{d\sigma_e(E, \theta)}{d\Omega} \sin \theta \frac{d\theta}{\sigma_e}. \quad (4)$$

The azimuthal angle after the elastic collision is selected by another random number  $R_2 \in (0, 1)$ :

$$\phi = 2\pi R_2. \quad (5)$$

The mean free path for elastic scattering  $\lambda_e$  is given by

$$\lambda_e = \frac{A}{N_a \rho \sigma_e}, \quad (6)$$

where  $A$  is the atomic weight of the target material,  $\rho$  is the density, and  $N_a$  is the Avogadro's number.

## 2.2 Inelastic Scattering

The inelastic processes considered in this model are ionization of core and conduction electrons, and plasmon excitation. The excitation of core electrons is described using the differential cross section developed by Gryzinski:<sup>10)</sup>

$$\begin{aligned} \frac{d\sigma_{ic}(\Delta E, E)}{d(\Delta E)} &= N_B \pi e^4 \frac{1}{(\Delta E)^3} \frac{E_B}{E} \left( \frac{E}{E+E_B} \right)^{3/2} \left( 1 - \frac{\Delta E}{E} \right)^{E_B/(E_B+\Delta E)} \\ &\times \left\{ \frac{\Delta E}{E_B} \left( 1 - \frac{E_B}{E} \right) + \frac{4}{3} \ln \left( 2.7 + \sqrt{\frac{E-\Delta E}{E_B}} \right) \right\}, \end{aligned} \quad (7)$$

where  $\Delta E$  is the energy transferred from the primary electron to the bound electron,  $E_B$  is the binding energy of the core electron, and  $N_B$  is the occupation number of electrons in the  $ic$  shell. The total ionization cross section  $\sigma_{ic}(E)$  is obtained by integrating Eq. (7) over all possible values of  $\Delta E$ :<sup>1)</sup>

$$\begin{aligned} \sigma_{ic} &= \pi e^4 N_B \frac{1}{E_B^2} \frac{E_B}{E} \left( \frac{E-E_B}{E+E_B} \right)^{3/2} \left\{ 1 + \frac{2}{3} \left( 1 - \frac{E_B}{2E} \right) \right. \\ &\times \left. \ln \left( 2.7 + \sqrt{\frac{E-\Delta E}{E_B}} \right) \right\}. \end{aligned} \quad (8)$$

The energy-loss of the primary electron resulting from an inelastic scattering with the  $ic$  shells is determined using random number  $R_3 \in (0, 1)$  and by finding a value of  $\Delta E$  which satisfies the relation

$$R_3 = \int_{E_B}^{\Delta E} \frac{d\sigma_{ic}(\Delta E', E)}{d\Delta E} \frac{d\Delta E'}{\sigma_{ic}(E)}. \quad (9)$$

The energy of a conduction electron excited by the primary electron,  $E_S$ , is assumed to have a distribution approximated by the Streitwolf's excitation function,<sup>11)</sup> which is given by

$$S(E_S) = \frac{e^4 k_f^3}{3\pi E(E_S - E_F)^2}, \quad (10)$$

where  $E$  is the energy of the primary electron,  $E_F$  is the Fermi energy, and  $k_f$  is the wave vector

corresponding to the Fermi energy.

In Eq. (10),  $S(E_S)$  is the number of secondary electrons excited per unit energy into an energy interval between  $E_S$  and  $E_S + dE_S$  per unit path length of the primary electron. In a practice this energy distribution is obtained by numerically by using random number  $R_4 \in (0, 1)$ . The secondary electron energy,  $E_S$ , is given by the following equation:

$$R_4 = \int_{E_c}^{E_S} \frac{S(E_S)}{dE_S} \frac{dE_S'}{\sigma_c(E_S)}. \quad (11)$$

where  $E_c = E_F + \Phi$ ,  $\Phi$  is the work function, and  $\sigma_c(E_S)$  can be written by

$$\sigma_c(E_S) = \frac{e^4 k_f^3}{3\pi E} \frac{E - E_F - \Phi}{\Phi(E - E_F)}. \quad (12)$$

We have used this function because it is a simple and reasonably accurate expression consistent with the level of approximation used to represent the other inelastic events. The same function has been successfully used by other workers.<sup>1)</sup>

In the case of core and conduction electron excitation, the angular distribution of primary and created secondary electrons after the inelastic collision is estimated by the classical binary collision model.<sup>10)</sup> The energy of the primary electron after the collision is written as

$$E' = E \cos^2 \theta, \quad (13)$$

where  $\theta$  is the scattering angle.

The energy of the created secondary electron is given by

$$E'' = E \sin^2 \theta, \quad (14)$$

where  $E' = E$  or  $E_S$  depending on the observed inelastic process.

The expression of the mean free path for the excitation of bulk plasmons of energy  $E_{pl}$  is derived by Quinn:<sup>12)</sup>

$$\lambda_{pl} = \frac{2a_0 E}{E_{pl}} \ln \left[ \frac{(E_F + E_{pl})^{1/2} - E_F^{1/2}}{E^{1/2} - (E - E_{pl})^{1/2}} \right]. \quad (15)$$

The differential cross section for the scattering angle of an electron which excites a plasmon is given by

$$\frac{d\sigma_{pl}(E, \theta)}{d\Omega} = \frac{1}{2\pi n_0 a_0} \frac{\Theta_E}{\Theta^2 + \Theta_E^2}, \quad (16)$$

where  $n_0$  is the free electron density and  $\Theta_E = E_{pl}/2(E - E_F)$ . The energy loss of an primary electron after the bulk plasmon excitation is equal to  $E_{pl}$ .

From Eq. (16) we obtain the following expression for an polar scattering angle as a function of  $R_5 \in (0, 1)$  random number:

$$\Theta = \Theta_E \sqrt{\exp \left( R_5 \ln \frac{2 + \Theta_E}{\Theta_E} \right) - 1}. \quad (17)$$

The azimuthal angle after all inelastic collisions is determined by Eq. (5). The same formalism is used in the case of surface plasmon excitation with energy  $E_{pl}/\sqrt{2}$  as in a bulk plasmon excitation. The mean free path for the inelastic scattering process,  $\lambda_{in}$ , is related to the partial mean free path for the different inelastic scattering processes by

$$\frac{1}{\lambda_{in}} = \frac{1}{\lambda_c} + \frac{1}{\lambda_v} + \frac{1}{\lambda_{pl}}, \quad (18)$$

where  $\lambda_c, \lambda_v$ , and  $\lambda_{pl}$  are the mean free paths for core electron, valence electron and plasmon

excitation, respectively.

### 2.3 Computation Procedures

Figure 2 shows the flow diagram of the MC program which simulates the primary electron

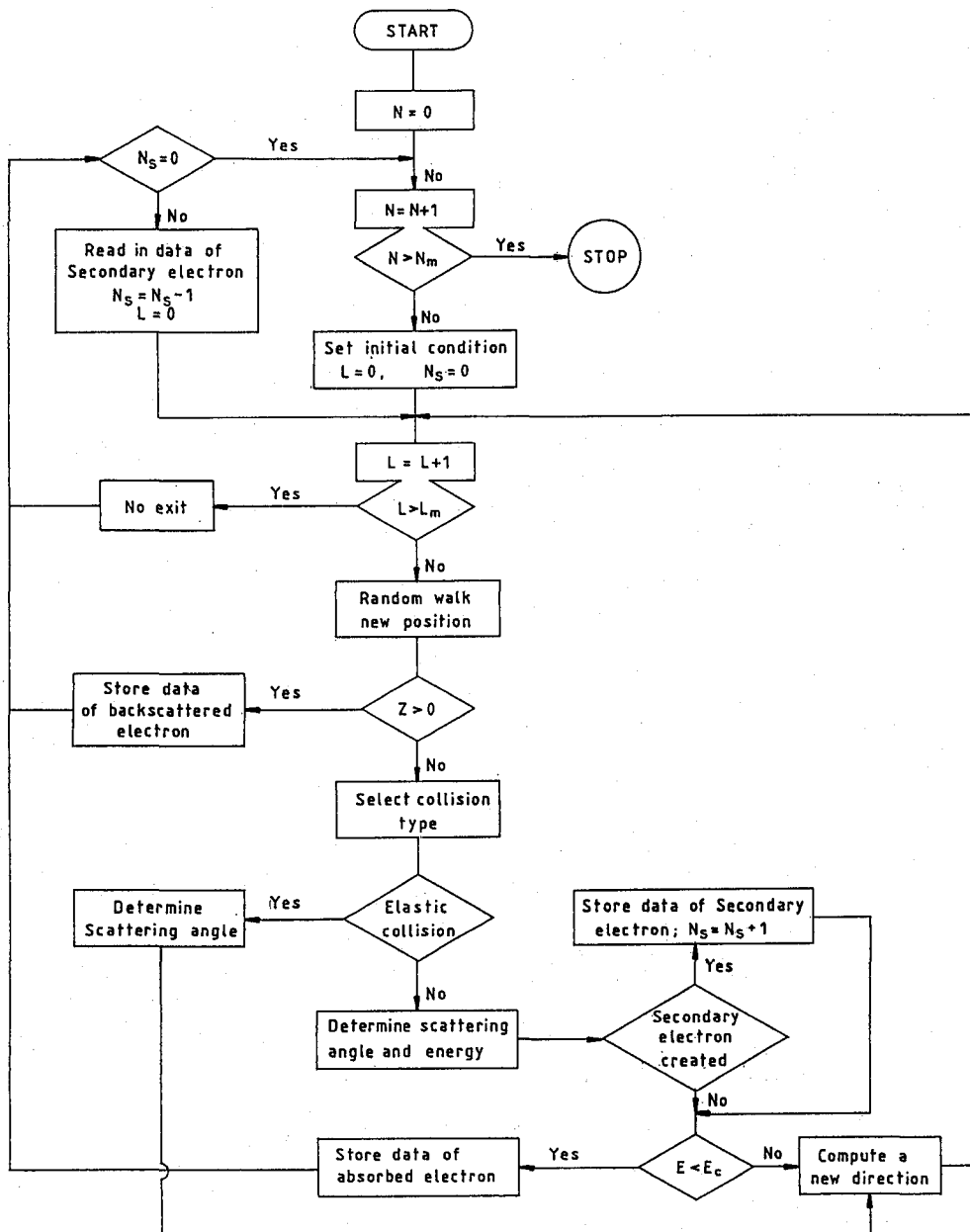


Fig. 2. Flow diagram of the Monte Carlo program. The symbols  $N$  and  $L$  denote the number of traced electrons and the number of steps of the tracing electron, respectively,  $N_m$  and  $L_m$  are their maximum values,  $N_s$  is the number of secondary electrons,  $z$  is the depth of the tracing electron,  $E$  is the kinetic energy of the electron, and  $E_c$  is the cut off energy.

and secondary electron trajectories in solids. The total average mean free path between scattering events,  $\lambda_{tot}$ , is defined by

$$\frac{1}{\lambda_{tot}} = \frac{1}{\lambda_e} + \frac{1}{\lambda_{in}}. \quad (19)$$

The path length  $s$  between any two scattering events has the Poisson distribution

$$P(s) = \lambda_{tot}^{-1} e^{-s/\lambda_{tot}}, \quad (20)$$

and can be obtained with a uniform random number  $R_7 \in (0, 1)$  via the relation

$$s = -\lambda_{tot} \ln(R_7). \quad (21)$$

The type of scattering for each scattering event is selected by using a random number  $R_8$  according to the relation

$$\lambda_{tot} \sum_{i=1}^j \frac{1}{\lambda_{i-1}} \leq R_8 \leq \lambda_{tot} \sum_{i=1}^j \frac{1}{\lambda_i}, \quad (22)$$

where  $j$  denotes the type of scattering (i.e. elastic, conduction band, core electron or plasmon).

The scattering angles,  $\vartheta$  and  $\varphi$ , are referenced to the local coordinate system of the electron just before the scattering event (see Fig. 1) and must be converted into the coordinate system of the laboratory according to the following relations:<sup>13)</sup>

$$\cos \theta_n = \cos \theta_{n-1} \cos \vartheta + \sin \theta_{n-1} \sin \vartheta \cos \varphi, \quad (23)$$

$$\cos(\phi_n - \phi_{n-1}) = \frac{\cos \vartheta - \cos \theta_n \cos \theta_{n-1}}{\sin \theta_{n-1} \sin \theta_n}, \quad (24)$$

$$\sin(\phi_n - \phi_{n-1}) = \frac{\sin \vartheta \sin \varphi}{\sin \theta_n}, \quad (25)$$

where  $\theta_{n-1}$  and  $\phi_{n-1}$  denote the direction of motion of an electron before scattering and  $\theta_n, \phi_n$  are its direction just after scattering through the scattering angle of  $\vartheta$  and  $\varphi$  being the azimuthal scattering angle. The electron goes forward one step with a defined orientation and its position at the next scattering point is given by the equation:

$$\begin{pmatrix} x_{n+1} \\ y_{n+1} \\ z_{n+1} \end{pmatrix} = \begin{pmatrix} x_n \\ y_n \\ z_n \end{pmatrix} + s_n \begin{pmatrix} \sin \theta_n \cos \phi_n \\ \sin \theta_n \sin \phi_n \\ \cos \theta_n \end{pmatrix}. \quad (26)$$

We have made an assumption in the simulation that an electron transverses the first stop,  $s_0$ , without scattering at the sample vacuum interface, as shown in Fig. 1. The terminal point of the first flight is the first scattering point. The flow diagram of the code is given in Fig. 2. First, a primary electron trajectory is simulated and all the parameters (energy, position, and scattering angle) of produced secondary electrons by the primary electron in core and conduction band excitation events are stored. After completion of tracing the primary electron, all the stored data on the secondary electrons are recalled and their trajectories are simulated in the same way as for the primary electron. This cascade process is continued until all electrons either escape from the solid by backscattering or come to rest within the sample. It should be noted that we introduce one more channel, the so-called anomaly trajectory, for the end of history. This situation corresponds to the case when the electron neither escapes nor stops and the number of steps to trace electrons exceeds a certain maximum value.

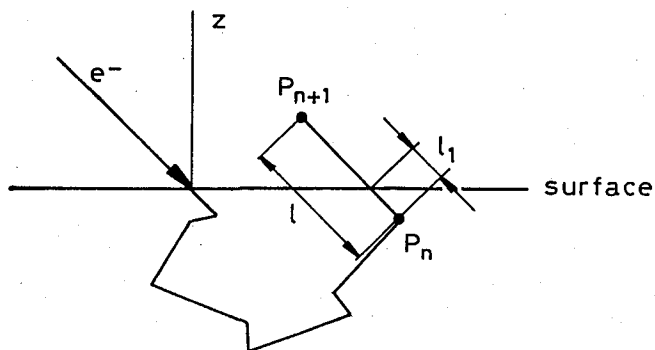


Fig. 3. Scheme showing the energy-loss correction for the emerging electron.

When the electron emerges from the solid surface, the energy-loss correction is made if the final scattering event is a core or conduction band excitation process (see Fig. 3). The energy-loss of the escaping electron by the last collision is defined as

$$\Delta E^{last} = \Delta E \frac{l_1}{l}, \quad (27)$$

where  $l$  is the distance between the final point of the calculated trajectory and the last scattering position in the specimen,  $l_1$  is the distance between the solid surface and the last scattering position, and  $\Delta E$  is the calculated energy-loss of the electron during the last inelastic process.

### 3. RESULTS AND DISCUSSION

Based on the computational method described above, a computer code to trace the electron penetration in solids has been written. All the numerical computations in the present work have been performed on the CRAY Y-MP2E supercomputer in the Institute for Chemical Research, Kyoto University.

In order to test the present code, the energy distribution of electrons backscattered from the amorphous Al was calculated and compared with the experimental spectrum. The backscattered electron spectrum near the elastic peak was measured with an electrostatic electron spectrometer at the Institute of Nuclear Research of the Hungarian Academy of Sciences (ATOMKI).<sup>15)</sup> The energy of the primary electron beam was 5 keV and the incident angle of the beam was 36°.

In the present calculation, the binding energies of K and L shells in Al were taken to be 1560 and 84.5 eV, respectively. The occupation number of core electrons is assumed to be 2 for K shell and 8 for L shell. In order to obtain the fine structures near the elastic peak of the backscattered electrons, a large number of histories of the incident electrons are necessary. We simulated  $10^6$  primary electron trajectories in the present work.

Figure 4 shows the comparison between the calculated and measured electron spectra. The calculated distribution of the backscattered electrons was convoluted with the finite relative energy resolution of the electron spectrometer, ( $\Delta E/E=0.035\%$ ). It is clear from the figure that the calculated spectrum agrees well with the measured one both in magnitude and in shape of the electron peaks. In the figure, the plasmon loss peaks appear on the low energy side of the elastic peak located at 5000 eV. The slight discrepancy between the calculated and measured positions

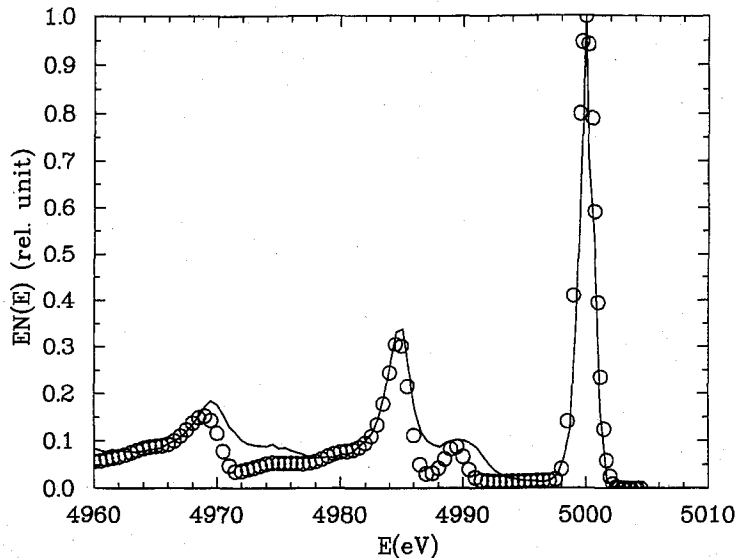


Fig. 4. Electron spectra backscattered from the amorphous aluminum sample near the elastic peak: — measured by Némethy *et al.* (Ref. 15); ○ calculated (The spectrum was convoluted for finite relative energy resolution,  $E=5$  keV and  $\Delta E/E=0.035\%$ .)

of the plasmon loss peaks can be ascribed to the difference between the calculated and measured plasmon energies.

In conclusion, we have developed the MC code for electron transport in solids, based on several scattering models. To demonstrate the validity of the approximations used in the present code, the calculation of the energy spectrum of backscattered electrons from Al was performed and the obtained result was compared with the experimental data. It is confirmed that the calculated energy distribution can well reproduce the fine structures in the measured spectrum near the elastic peak. This fact indicates that the present MC code is useful to estimate electron transport in solids.

#### ACKNOWLEDGEMENTS

The authors would like to thank the Supercomputer Laboratory, Institute for Chemical Research, Kyoto University, for providing them computer time. One of us (K.T.) thanks for the kind hospitality during his stay in Institute for Chemical Research, Kyoto University, and wishes to thank Professor R. Shimizu for valuable discussion. This work was performed under the Japanese-Hungarian Cooperative Research Project and partially supported by the research projects: OTKA/TOO 7274/1993 (Hungarian).

#### REFERENCES

- (1) R. Shimizu, Y. Kataoka, T. Ikuta, T. Koshikawa and H. Hashimoto, *J. Phys. D: Appl. Phys.*, **9**, 101 (1976).
- (2) F. Salvat, J.D. Martinez, R. Mayol and J. Parellada, *J. Phys. D: Appl. Phys.*, **18**, 299 (1985).
- (3) J.D. Martinez, R. Mayol and F. Salvat, *J. Appl. Phys.*, **67**, 2955 (1990).



- (4) A. Desalvo, A. Parisini and R. Rosa, *J. Phys. D: Appl Phys.*, **17**, 2455 (1984).
- (5) A. Desalvo and R. Rosa, *J. Phys. D: Appl Phys.*, **20**, 790 (1987).
- (6) M. Kotera, K. Murata and Nagami, *J. Appl. Phys.*, **52**, 997 (1981).
- (7) Z.J. Ding and R. Shimizu, *Surf. Sci.*, **222**, 313 (1989).
- (8) Z.J. Ding and R. Shimizu, *Surf. Sci.*, **197**, 539 (1988).
- (9) M.J. Berger, in "Methods in Computational Physics," ed. by B. Alder, S. Fernback and M. Rotenberg, Academic, New York, p. 135 (1963).
- (10) M. Gryzinski, *Phys. Rev.*, **138**, A336 (1965).
- (11) H.W. Streitwolf, *Ann. Phys. (Leipzig)*, **3**, 183 (1959).
- (12) J.J. Quinn, *Phys. Rev.*, **126**, 1453 (1962).
- (13) G. Wenzel, *Z. Physik*, **40**, 590 (1927).
- (14) W. Jr. Williamson and G.C. Duncan, *Am. J. Phys.*, **54**, 262 (1986).
- (15) A. Némethy, L. Kövér and D. Varga, private communication.